The Bethe-Salpeter Equation (BSE) and Unitarization of ChpT - Amplitudes

C. García-Recio
J.N.
E. Ruiz Arriola

University of Granada

Spain

M.J. Vicente-Vacas

University of Valencia + IFIC

NP-2002

Introduction + CONCLUSIONS

- N^* Resonances $\overset{?}{\Longleftarrow}$ QCD.
  - Renorm. Theory of quarks and gluons.
  - Non-perturbative at low energies.
- Lattice QCD
- ChpT : Effective Field Theory
  - * Low energy Physics DOES NOT depend on details of the short distance dynamics, but rather on some bulk properties effectively encoded in the **LOW ENERGY PARAMETERS**
  - * Relevant degrees of freedom : HADRONS and not QUARKS & gluons. CONNECTION to the underlying QCD Dynamics becomes obscure
  - * Resonances ← Unitarity (non-perturbative)

Meson-Baryon Scattering

ChpT only satisfies Unitarity perturbatively ⇒

How can we restore exact Unitarity?

MODEL DEPENDENT !!

BSE:

+ ...

"Sum of bubbles"

Input: V Two particle irreducible amplitude propagators.

- Exact.
- $\forall$ V → T (exact) fullfils two particle unitarity.
- ChpT → TRUNCATE BSE.

New Expansion patterns !!!

- Requires Renormalization ⇒

UNDERTERMINED ← LOW ENERGY PARAMETERS (↑ M. Ludwig, Kolomeitsev)

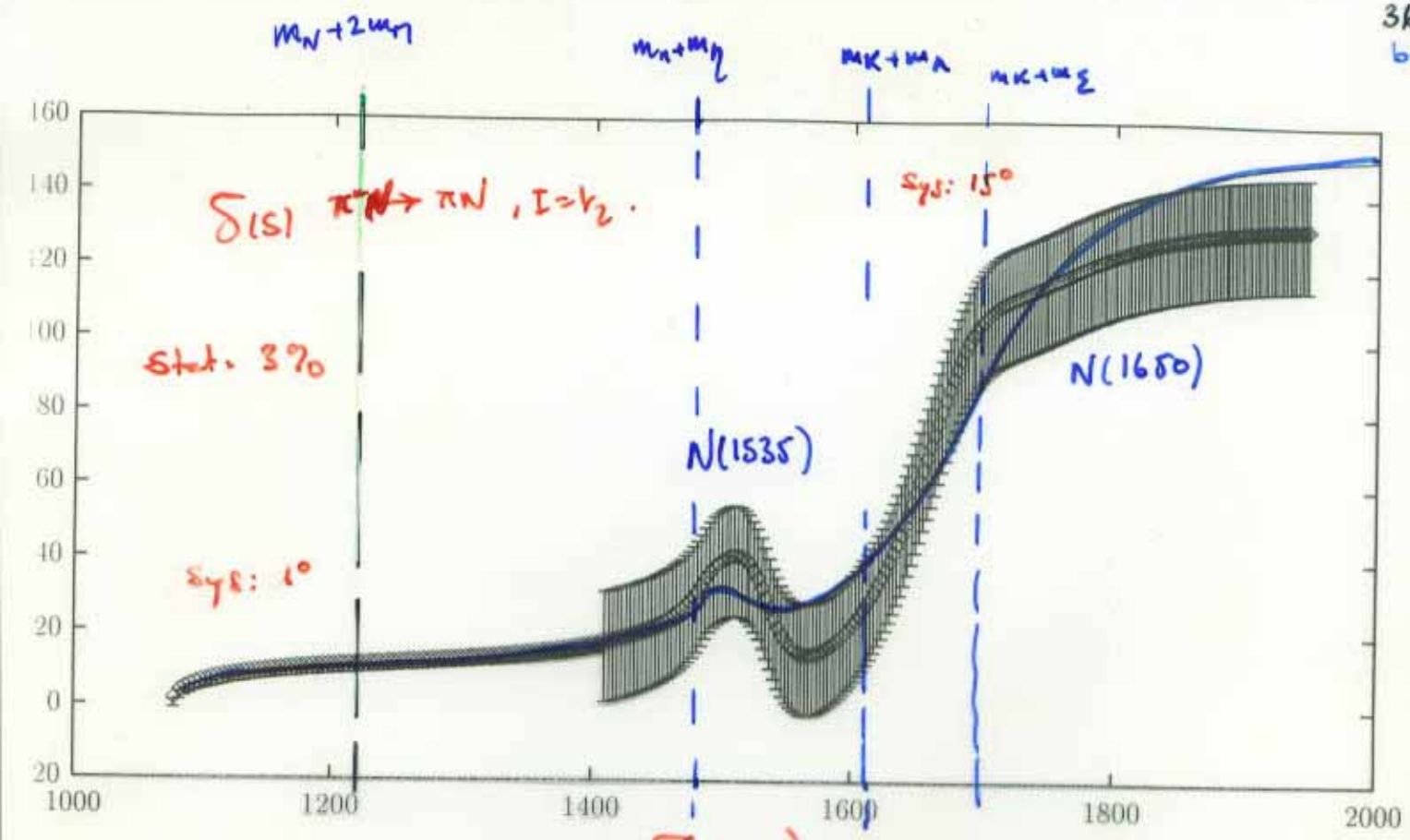

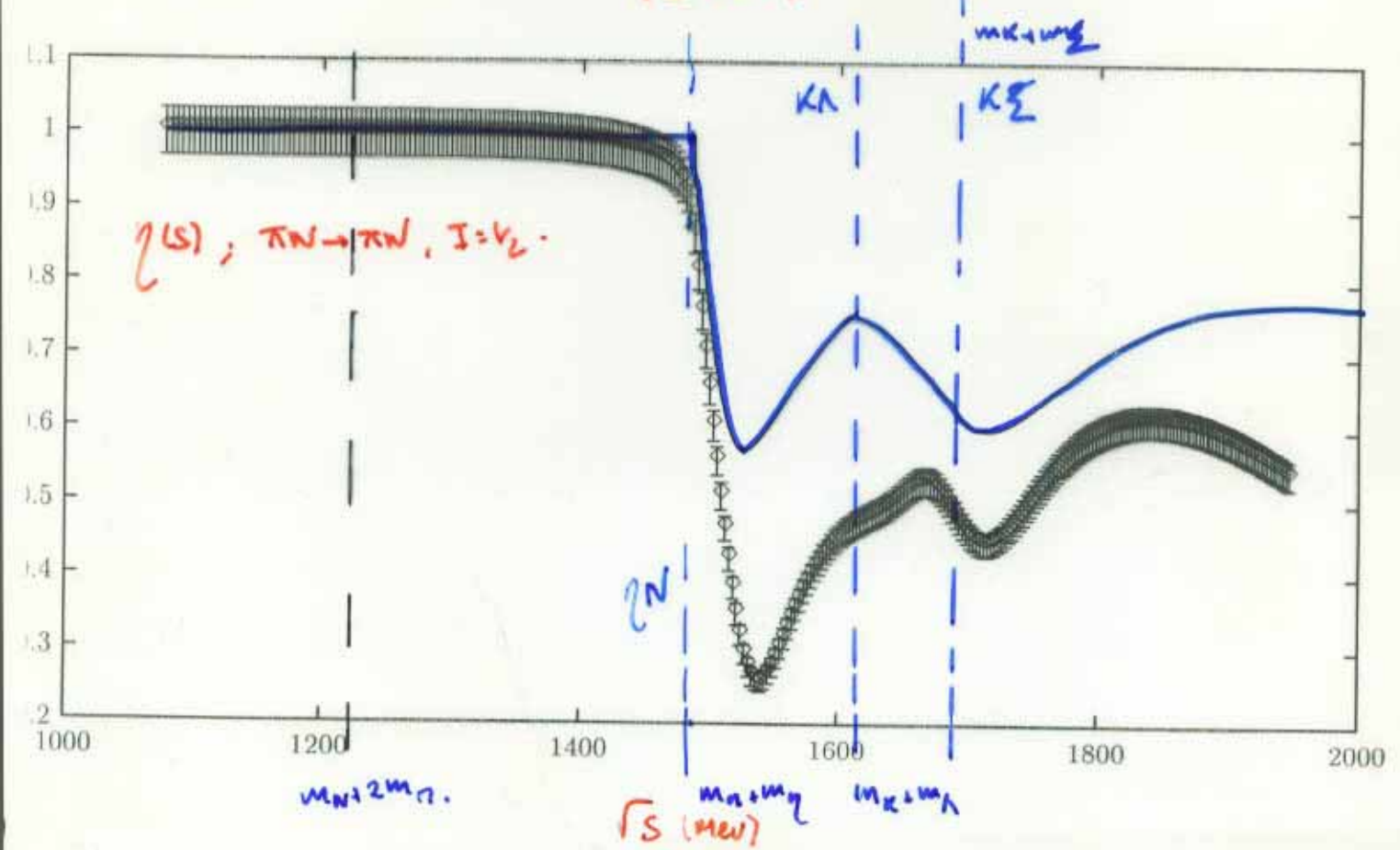

$$\sigma_{inel} \propto 1-\eta^2 = \sigma_{\pi N \to \pi N} + \sigma_{\pi N \to \eta N} + \sigma_{\pi N \to K\Lambda} + \sigma_{\pi N \to K\Sigma} +$$

$$+ \sigma_{\pi N \to \pi\pi N}$$

πN Unitarized coupled channel chiral Perturbation Theory

PRD64 (2001) 116008

$\Rightarrow$ Strangness $S=0$.

$\Rightarrow$ $I=1/2$, $J=\frac{1}{2}$, $P=-$, $L=0$.

PDG: Resonances:

N(1535)
- Breit-Wigner mass = 1520 - 1555 MeV.
- " width = 100 - 250 MeV.
- Re (pole position) = 1495 - 1515 MeV
- -2 Im (pole position) = 90 - 250 MeV.

Decay Modes: $N\pi$ 35-55%; $N\eta$ 30-55%; $N\pi\pi$ 1-10%

N(1650)
- BW mass 1640 - 1680 MeV.
- BW width 140 - 180 MeV.
- Re (pole position) 1640 - 1670 MeV
- -2 Im (pole position) 150 - 170 MeV.

Decay Modes: $N\pi$ 55% - 90%; $N\eta$ 3 - 10%; ΛK 3 - 11%; $N\pi\pi$ 10 - 20%

Three body channel

Second Riemann sheet.

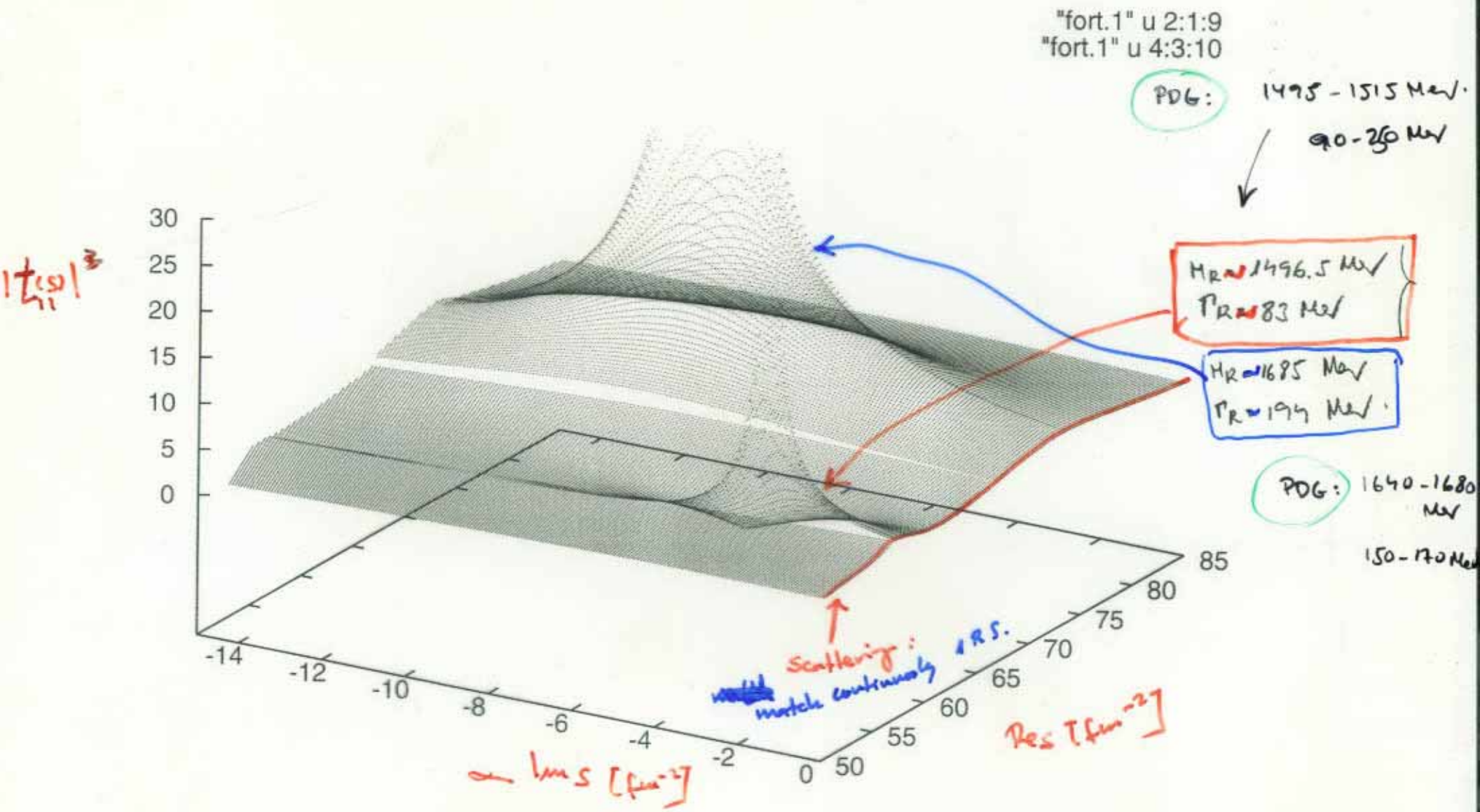

Chiral Baryon-Meson Lagrangian.

$\Rightarrow$ Lowest order

$$\mathcal{L}_1 = \mathrm{Tr}\left\{ \bar{B}\left(i\not{\nabla} - \hat{M}\right) B \right\} + \frac{1}{2} D\, \mathrm{Tr}\left\{ \bar{B}\gamma^\mu\gamma_5 \{u_\mu, B\} \right\} + \frac{1}{2} F\, \mathrm{Tr}\left\{ \bar{B}\gamma^\mu\gamma_5 [u_\mu, B] \right\}.$$

$\mathrm{Tr} = \mathrm{Tr}^{SU(3)}$

$$\nabla_\mu B = \partial_\mu B + \frac{1}{2}\left[u^+\partial_\mu u + u\partial_\mu u^+, B\right]$$

$$U = u^2 = e^{i\sqrt{2}\Phi/f}, \quad u_\mu = i u^+ \partial_\mu U u^+$$

$F \sim 0.46$, $D \sim 0.79$ $\left\{ (F+D = g_A = 1.25) \right.$

$$\Phi = \begin{pmatrix} \frac{\pi^0}{\sqrt{2}} + \frac{1}{\sqrt{6}}\eta & \pi^+ & K^+ \\ \pi^- & -\frac{1}{\sqrt{2}}\pi^0 + \frac{1}{\sqrt{6}}\eta & K^0 \\ K^- & \bar{K}^0 & -\frac{2}{\sqrt{6}}\eta \end{pmatrix}$$

$$B = \begin{pmatrix} \frac{\Sigma^0}{\sqrt{2}} + \frac{\Lambda}{\sqrt{6}} & \Sigma^+ & p \\ \Sigma^- & -\frac{1}{\sqrt{2}}\Sigma^0 + \frac{\Lambda}{\sqrt{6}} & n \\ \Xi^- & \Xi^0 & -\frac{2}{\sqrt{6}}\Lambda \end{pmatrix}$$

The MB → MB vertex obtained from the former Lagrangian reads:

$$\mathcal{L}_{MB\to MB} = \frac{i}{4f^2} \mathrm{Tr}\{\bar{B}\gamma^\mu [[\Phi, \partial_\mu \Phi], B]\}.$$

Scattering amplitude T at lowest order is given by

$$t_I^{(1)}(K,K') = \frac{D}{f^2}(\not{K} + \not{K}')$$

K, K' meson in and out momenta.

$$D = \frac{1}{4}\begin{pmatrix} -2 & 0 & -3/2 & 1/2 \\ 0 & 0 & 3/2 & 3/2 \\ -3/2 & 3/2 & 0 & 0 \\ 1/2 & 3/2 & 0 & -2 \end{pmatrix} \begin{matrix} \pi N \\ \eta N \\ K\Lambda \\ K\Sigma \end{matrix}$$

$\pi N \quad \eta N \quad K\Lambda \quad K\Sigma$

Normalization.

$T = 1/2$

$$B(M_A, P-K, s_A) + M(m_A, K) \to B(M_B, P-K', s_B) + M(m_B, K')$$

P: Total CM momentum.
K's: meson momenta

$M_{A,B}$ } masses
$m_{A,B}$ }

$s_{A,B}$ ≡ spin indices

$$\text{CM} \to \frac{d\sigma}{d\Omega}[B \leftarrow A] = \frac{1}{64\pi^2 s}\frac{|\vec{K}_B|}{|\vec{K}_A|}\left|T_P[B\{K_B, s_B\} \leftarrow A\{K_A, s_A\}]\right|^2$$

$$\to T_P[B\{K', s_B\} \leftarrow A\{K, s_A\}] =$$

$$\bar{u}_B(P-K', s_B)\, t_P(K, K')\, u_A(P-K, s_A)$$

$t_P(K,K')$: matrix in both { Dirac, coupled channel } spaces.

On the mass shell

$$t_P(K,K')\big|_{\text{on-shell}} = t_1(s,t)\not{P} + t_2(s,t)$$

matrices in the coupled channel.

$s = P^2$
$t = (K-K')^2$

$\Rightarrow$ s-wave coupled channel matrix $f_0^{1/2}(s)$ is given by

$$\left[f_0^{1/2}(s)\right]_{B \leftarrow A} = -\frac{1}{8\pi\sqrt{s}}\sqrt{\frac{|\vec{K}_B|}{|\vec{K}_A|}}\sqrt{E_B+M_B}\sqrt{E_A+M_A} \times$$

$$\times \int_{-1}^{+1} d\cos\theta \left(t_1(s,t) + t_2(s,t)\right)$$

$$\left[f_0^{V_2(S)}\right]_{AA} = \frac{1}{2i|\vec{K}_A|}\left(\eta_A e^{2i\delta_A} - 1\right)$$

η_A: inelasticities; $e^{2i\delta_A}$: phase-shifts

Optical Theorem

only open channels contribute.

$$\frac{4\pi}{|\vec{K}_A|}\,\mathrm{Im}\left[f_0^{V_2(S)}\right]_{AA} = \sum_B \sigma_{B\leftarrow A} =$$

$$= 4\pi \sum_B \left|\left[f_0^{V_2(S)}\right]_{BA}\right|^2 = \sigma_{AA} + \frac{\pi}{|\vec{K}_A|^2}\left(1-\eta_A^2\right)$$

Bethe-Salpeter Equation

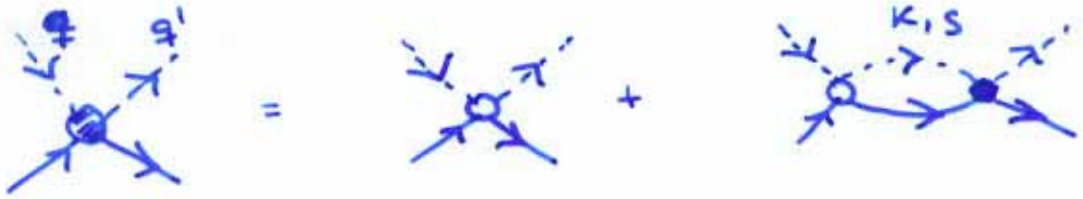

two particle irreducible amplitude (potential)

$$\left[t_I(q,q')\right]_{f\leftarrow i} = V_I(q,q')\Big|_{f\leftarrow i} +$$

$$+ i\int \frac{d^4K}{(2\pi)^4} \sum_{\substack{S=\pi N,\eta N \\ K\Lambda, K\Sigma}} t_I(K,q')\Big|_{f\leftarrow s} \left[\Delta(K)\, S(P-K)\right]_s \times$$

Exact pseudoscalar meson propagator. Exact baryon propag.

$$\times V_I(q,K)\Big|_{s\leftarrow i}.$$

- Exact Equation.
- The resulting scattering amplitude fulfills the coupled channel unitarity condition →

$$t_p(q,q') - \bar{t}_p(q',q) = -i(2\pi)^2 \int \frac{d^4K}{(2\pi)^4}\, t_I(K,q')\, \delta^+(K^2-\hat{m}^2)$$

$$(\not{P}-\not{K}+\hat{M})\,\delta^+\left[(P-K)^2-\hat{M}^2\right]\bar{t}_p(K,q).$$

$$\rightarrow \bar{t}_I(K,p) = \gamma^0 \underbrace{t_I^+(K,p)}_{\text{adjoin in the Dirac and coupled channel spaces.}} \gamma^0$$

$$\rightarrow \delta^+ = \theta(P^0)\,\delta.$$

→ Independent of $V_I(q,q')$ →

- It suggests an expansion (chiral) for $V_p(q,q')$!!

: Lowest order

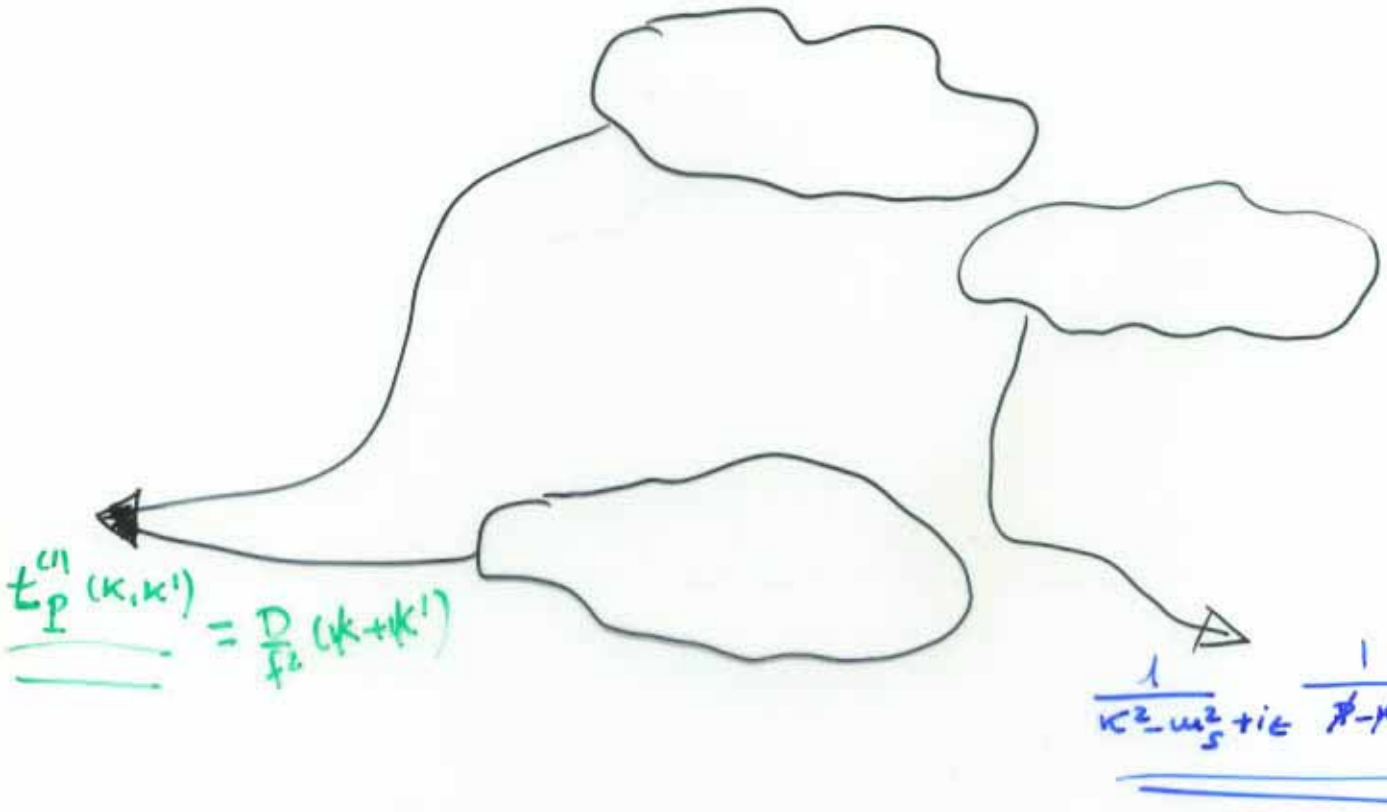

Exact solution: Solve a set of linear algebraic equations

↓

Remember

$$t_p(K,K')\Big|_{\text{on-shell}} = t_1(s,t)\,\not{p} + t_2(s,t)$$

at lowest order t_1, t_2 do not depend on t.

$$t(\not{p})^{-1} = -J(\not{p}) + \ldots\ldots \quad \text{real in the scatt. region.}$$

$$J(\not{p}) = i\int \frac{d^4q}{(2\pi)^4}\,\frac{1}{q^2-\hat{m}^2}\,\frac{1}{\not{P}-\not{q}-\hat{M}}.$$

→ Unitarity is restored.

$$\left[f_0^{\frac{1}{2}}(s)\right]_{BA} = -\frac{1}{8\pi\sqrt{s}}\sqrt{\frac{|\vec{K}_B|}{|\vec{K}_A|}}\sqrt{E_B+M_B}\sqrt{E_A+M_A}\;\; t(s)\Big|_{BA}$$

$$t(s) = t_1(s)\sqrt{s} + t_2(s).$$

MATRICES IN THE COUPLED-CHANNEL SPACE.

$$t_1 = (K_1 s - K_2 K_1^{-1} K_2)^{-1}$$

$$t_2 = (K_2 - K_1 K_2^{-1} K_1 s)^{-1}$$

$$K_1(s) = -\frac{s-\hat{m}^2+\hat{M}^2}{2s}J_0(s) + \frac{\Delta\hat{m}}{s-\hat{M}^2} - \frac{\Delta\hat{m}\hat{M}}{2s} + (\nu s - \mu\nu^{-1}\mu)^{-1}$$

$$K_2(s) = -\hat{M}J_0(s) + \frac{\hat{M}\Delta\hat{m}}{s-\hat{M}^2} - (\nu s\mu^{-1}\nu - \mu)^{-1}$$

$$\mu(s) = \frac{1}{f^4}\Big\{-[D,\hat{M}]\,\frac{\hat{M}\Delta\hat{m}}{s-\hat{M}^2}\,[D,\hat{M}] - f^2\{\hat{M},D\}_+ -$$

$$- D\Delta\hat{m}D\hat{M} + [D,\hat{M}]\Delta\hat{m}D\Big\}$$

$$\nu(s) = \frac{1}{f^4}\Big\{-[\hat{M},D]\,\frac{\Delta\hat{m}}{s-\hat{M}^2}\,[\hat{M},D] + D\Delta\hat{m}D + 2f^2D\Big\}.$$

where

$$J_0(s) = i\int \frac{d^4q}{(2\pi)^4}\,\frac{1}{q^2-\hat m^2}\,\frac{1}{(P-q)^2-\hat M^2} = \underbrace{\bar J_0(s)}_{\text{finite}} + \underbrace{J_0(s=(\hat m+\hat M)^2)}_{\text{divergent !!}}$$

logarithmically divergent

$$\bar J_0(s) \overset{s>(m+M)^2}{=} \frac{1}{(4\pi)^2}\left\{\left(\frac{M^2-m^2}{s} - \frac{M-m}{M+m}\right)\ln\frac{M}{m} + \frac{\lambda^{1/2}(s,m^2,M^2)}{s}\cdot\right.$$

$$\left.\cdot\left\{\log\frac{1+\sqrt{\frac{s-s_+}{s-s_-}}}{1-\sqrt{\frac{s-s_+}{s-s_-}}} - i\pi\right\}\right.$$

$s_+ = (m+M)^2$

$s_- = (m-M)^2$

diagonal matrix in the coupled channel space. In a given channel it reads.

$$2i\,\mathrm{Im}J_0(s) = 2i\,\mathrm{Im}\bar J_0(s) = J_0(s+i\epsilon) - J_0(s-i\epsilon) =$$

$$= -2i\,\frac{\lambda^{1/2}(s,m^2,M^2)}{16\pi s}\,\theta(s-s_+)\,.$$

diagonal matrix.

$$\Delta_{\hat m} = i\int\frac{d^4q}{(2\pi)^4}\,\frac{1}{q^2-\hat m^2}$$

$$\Delta_{\hat m\hat M} = i\int\frac{d^4q}{(2\pi)^4}\,\frac{1}{q^2-\hat m^2} - i\int\frac{d^4q}{(2\pi)^4}\,\frac{1}{q^2-\hat M^2}$$

→ quadratic divergences !!

$\hat M = \mathrm{diag}\,(M_N, M_N, M_\Lambda, M_\Sigma)$ $\qquad \hat m = \mathrm{diag}\,(m_\pi, m_\rho, m_K, m_K)$

Renormalization Constants (undetermined parameters)

$4 \longrightarrow f_0(s=(\hat{m}+\hat{H})^2)$
$4 \longrightarrow \Delta\hat{m}$
$4 \longrightarrow \Delta\hat{m}\hat{m}$
} diagonal

12 parameters $\Rightarrow$ from a best fit

$[f_0^{1/2}(s)]_{BA}$: 4×4 symetric matrix giving.

$\pi N \to \pi N$
$\eta N \to \eta N$
$K\Lambda \to K\Lambda$
$K\Sigma \to K\Sigma$
} elastic (η, δ)

$\pi N \to \eta N$
$\pi N \to K\Lambda$
$\pi N \to K\Sigma$
$\eta N \to K\Lambda$
$\eta N \to K\Sigma$
$K\Lambda \to K\Sigma$.
} inelastic. (σ)

Optical theorem, for instance

$$\left\{ \frac{4\pi}{p_{\pi N}} \left(\mathrm{Im}\, f_0^{1/2}(s)\right)_{\pi N\to\pi N} = \sigma^{el}_{\pi N} + \sigma_{\pi N\to\eta N} + \sigma_{\pi N\to K\Lambda} + \sigma_{\pi N\to K\Sigma} \right\}_{I=1/2}.$$

45 data points included in the best fit ($P_{lab} < 1.1$ GeV)

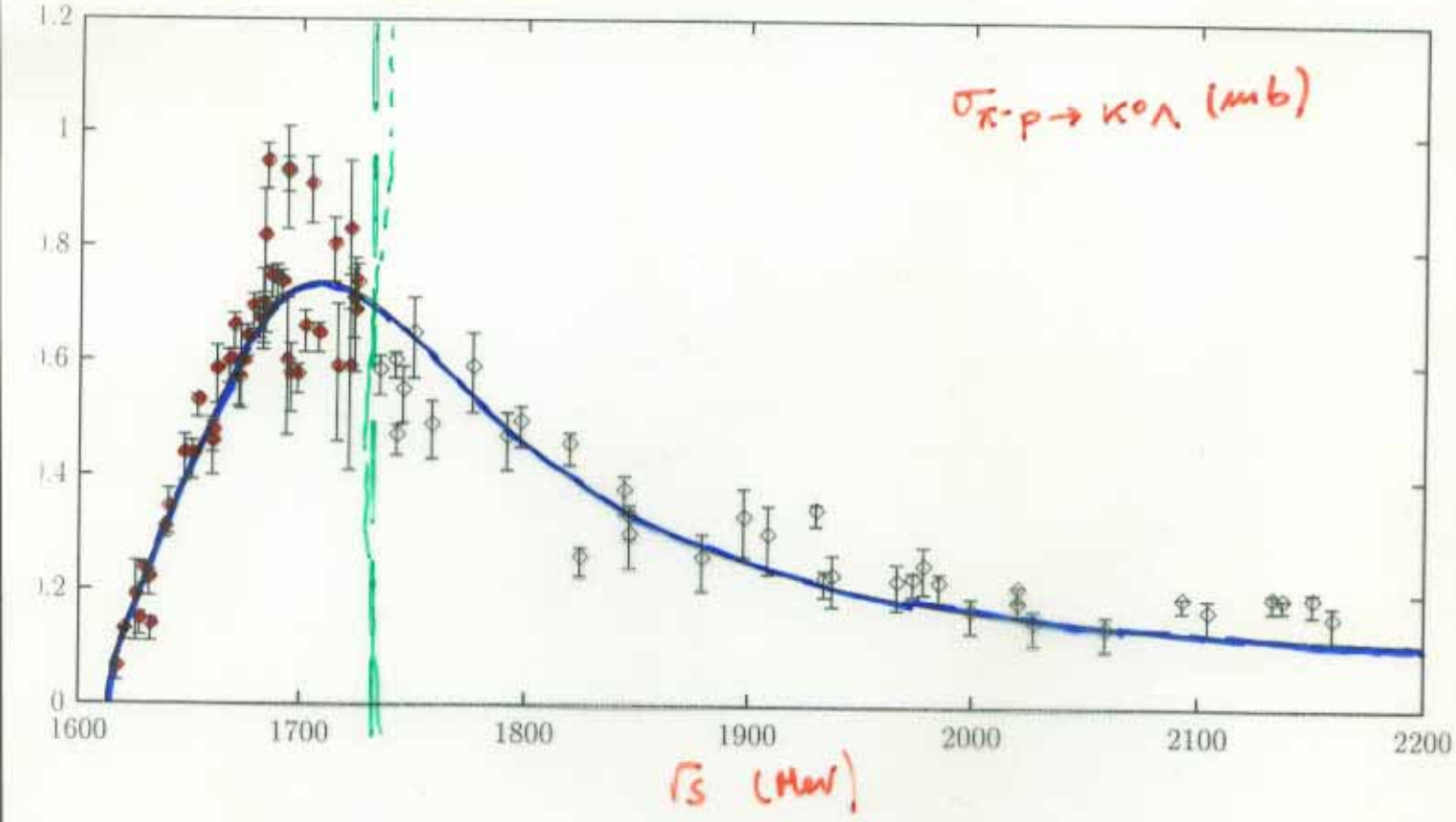

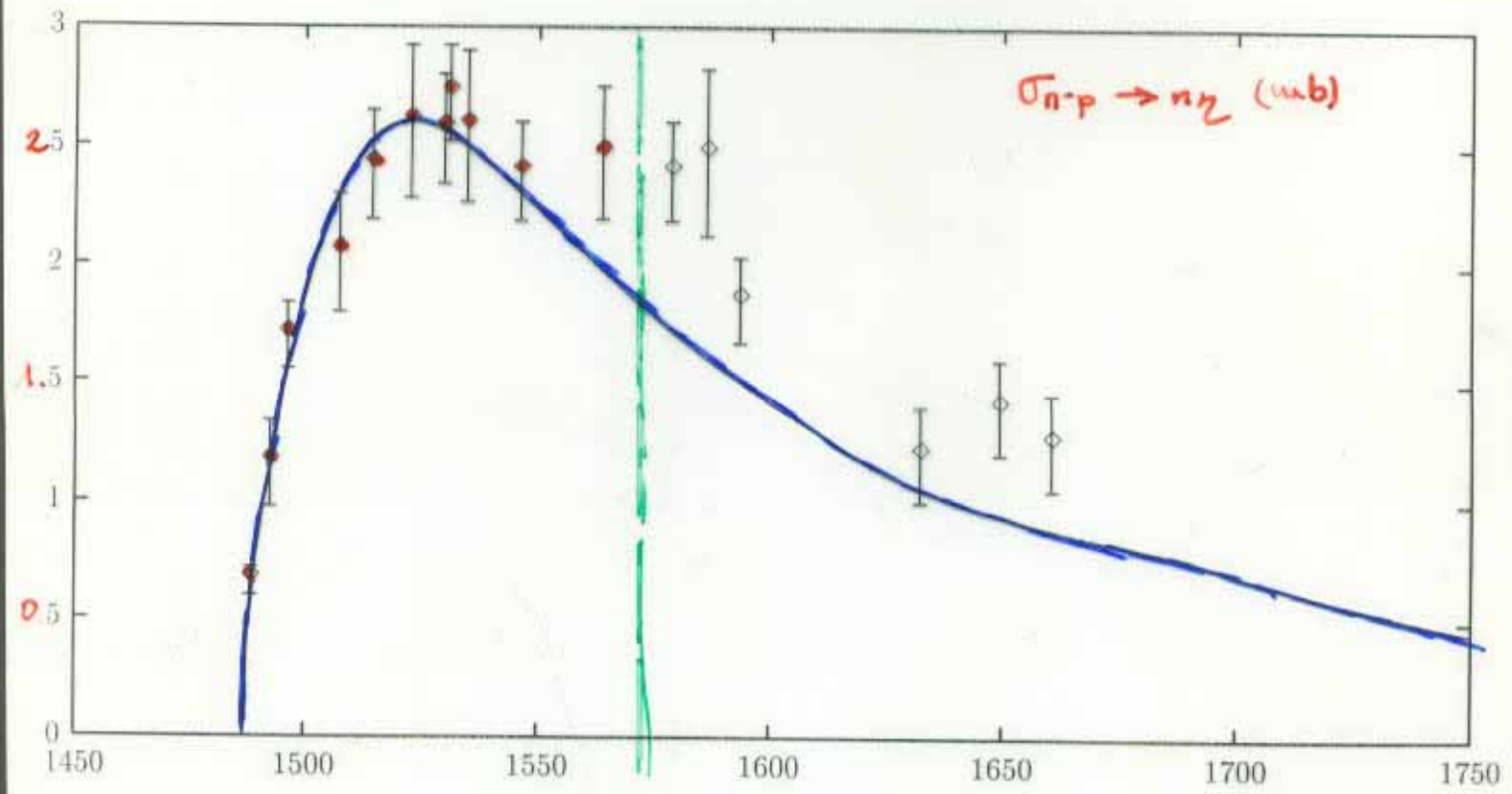

11 data points included in the best fit ($P_{lab} \leq 812$ MeV)

$a_{\eta N} = 0.772(5) + i\,0.217(3)$ fm

$a_{K\Lambda} = 0.0547(5) + i\,0.032(4)$ fm.

$L=0$

$I=1/2$

$J=1/2$

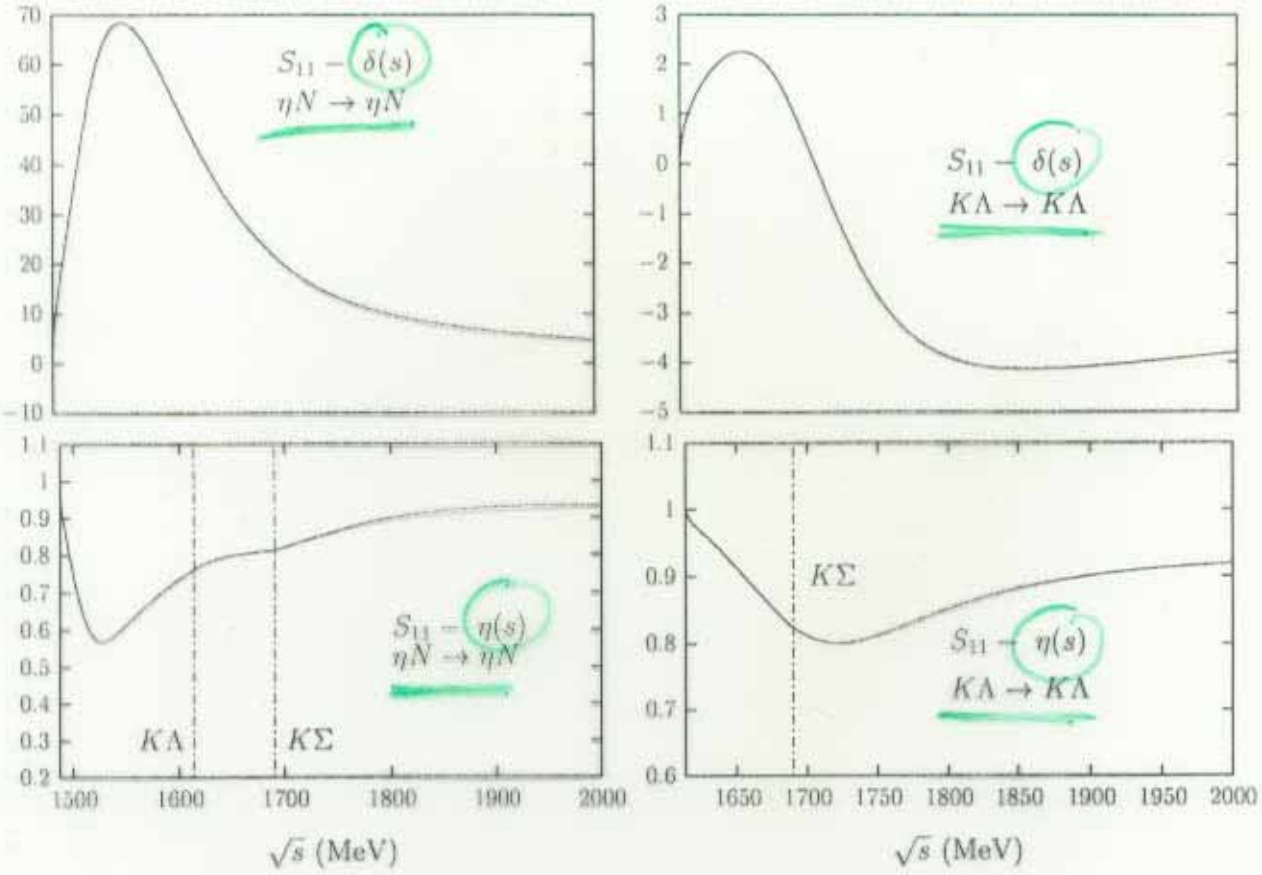

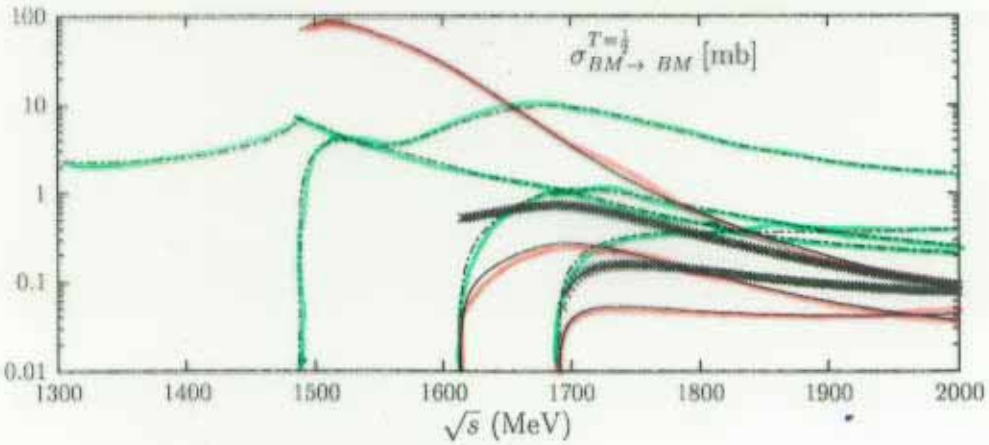

πN initial state.

ηN initial state.

$K\Lambda$ initial state.

FIG. 4. Top pannel: $s-$wave $T = 1/2$ phase shifts (in degrees) for elastic $\eta N \to \eta N$ (left pannel) and $K\Lambda \to K\Lambda$ (right pannel) processes as functions of the CM energy. Middle pannel: same as before but for inelasticities. Vertical lines indicate the opening of reaction thresholds. Bottom pannel: $s-$wave $T = 1/2$ meson-baryon cross sections ($\pi N \to \pi N, \eta N, K\Lambda, K\Sigma$; $\eta N \to \eta N, K\Lambda, K\Sigma$; $K\Lambda \to K\Lambda, K\Sigma$) in mbarns as functions of the CM energy. Dashed lines indicate πN initial state. Solid lines indicate ηN initial state. Crosses indicate $K\Lambda$ initial state. All the lines start at the relevant final state threshold (with the exception of the elastic $\pi N \to \pi N$ reaction).

place in the scattering line in the plot (upper lip of unitarity cut of the first Riemann sheet). We find three poles in the Second Riemann Sheet which positions are ($s = M_R^2 - iM_R\Gamma_R$):

$$\text{First Pole}: \quad M_R = 1368 \pm 12 \qquad \Gamma_R = 250 \pm 20 \tag{20}$$

$$\text{Second Pole}: \quad M_R = 1443 \pm 3 \qquad \Gamma_R = 50 \pm 7 \tag{21}$$

$$\text{Third Pole}: \quad M_R = 1677.5 \pm 0.8 \qquad \Gamma_R = 29.2 \pm 1.4 \tag{22}$$

where all units are given in MeV and errors have been transported from those in the best fit parameters (Eq. (A1)), taking into account the existing statistical correlations through a Monte–Carlo simulation.

These poles are related to the two S_{01} resonances $\Lambda(1405)$ and $\Lambda(1670)$ which appear up to this range of energy in the PDG (Ref. [33]). The third pole above can be clearly identified to the $\Lambda(1670)$ which is located at

$$\begin{aligned} \Lambda(1670): \quad & M_R = 1670 \pm 10 \quad \Gamma_R = 35^{+15}_{-10} \quad \text{Ref. [33]} \\ & M_R = 1673 \pm 2 \quad \Gamma_R = 23 \pm 6 \quad \text{Ref. [31]} \end{aligned} \tag{23}$$

where again units are in MeV. The agreement of our predictions and the experimental data is satisfactory and better than the previous theoretical LSE approach of Ref. [18]. Let us look at the $\Lambda(1405)$ resonance, following the PDG it is placed at (in MeV)

$$\Lambda(1405): \quad M_R = 1406.5 \pm 4.0 \qquad \Gamma_R = 50 \pm 2 \qquad \text{Ref. [33]} \tag{24}$$

Our amplitudes have two poles in the region of 1400 MeV, Eqs. (20) and (21). The features of the second one are in agreement with the previous results of Refs. [17,18] and though the width compares well with the experiment, the mass is shifted to higher values. Besides, we should note that the pole quoted in Eq. (20) is very broad and can not be identified with any of the experimentally established resonances. This pole is also present in the LSE model of Refs. [17,18], as it was pointed out in Ref. [34], though the mass position there is similar ($M_R = 1390$ MeV), the width is about a factor two narrower ($\Gamma_R = 132$ MeV) than ours. Our understanding is that this broad resonance does not influence strongly the scattering line. However, the $\pi\Sigma$ mass spectrum peaks around 1405 MeV in the experimental data and also in our approach as can be seen in Fig. 1. This is a clear indication of a sizeable non resonant contribution on top of our 1443 MeV pole.

On the other hand, there are unphysical poles in the physical (first) Riemann sheet. These unphysical poles appear because we have truncated the iterated potential to solve the BSE. The two of them closer to the scattering line are located at ($s = M^2 + iM\Gamma$) with $M \approx 1166$, $\Gamma \approx \pm 200$ MeV and $M \approx 1616$, $\Gamma \approx 631$ MeV. The tails of both poles can be seen in Fig. 4 and they do not influence the scattering line. In Appendix B, we will show the results from a fit which, at first sight, are even in a better agreement with the experimental data (Subsect. III A) than those presented up to now. However this apparent improvement is achieved because the unphysical poles get closer to real s axis and they affect, in a substantial manner, the scattering amplitudes. Hence, we discard this minimum, and we would like to note that it is important to observe the positions and influence of the unphysical poles when deciding the goodness of a phenomenological description of data.

Finally, we have also analyzed the nature of resonances on the light of the well known Breit-Wigner parameterization for coupled channels (See e.g. Ref. [35] and references therein),

$$t_{ij}^{\rm BW}(s) = -\frac{\delta_{ij}}{2i\rho_i}\left[e^{2i\delta_i} - 1\right] + \frac{e^{i(\delta_i+\delta_j)} M_R \sqrt{\Gamma_i^{\rm BW}\Gamma_j^{\rm BW}}}{\sqrt{\rho_i\rho_j}\left[s - M_R^2 + iM_R\Gamma_R\right]} \tag{25}$$

for which the background is assumed to be diagonal in coupled channel space and the relative phase of the resonance to the background and the sum partial decay widths, $\sum_i \Gamma_i^{\rm BW} = \Gamma_R$, are chosen in such a way that $t_{ij}^{\rm BW}(s)$ exactly fulfills unitarity on the real axis. The branching ratio is then defined as $B_i^{\rm BW} = \Gamma_i^{\rm BW}/\Gamma_R$. Subtracting the resonance contribution to the total amplitude, we have found that for our $\Lambda(1670)$ the background is not a diagonal matrix, since for our t_{ij}-matrix we get $2\sum_{i<j}|t_{ij} - t_{ij}^{\rm RBW}|^2 \approx \sum_i |t_{ii} - t_{ii}^{\rm RBW}|^2$ for $s \to M_R^2$, with $t_{ij}^{\rm RBW}$ the second term in Eq. (25). In addition, the BW parameterization suggests a relation between the residue at the pole and the imaginary part of the pole. This relation is only true in the sharp resonance approximation, $\Gamma_i^{\rm BW} << p_i$ with p_i the CM momentum of the decaying state. We have also checked that for our problem this is not the case. Actually, with such a definition we find that $\sum_i \Gamma_i^{\rm BW} \approx 0.8\Gamma_R$ for the $\Lambda(1670)$. This is a simple consequence of the incorrect assumption made by Eq. (25).

Reonances → Second Riemann Sheet

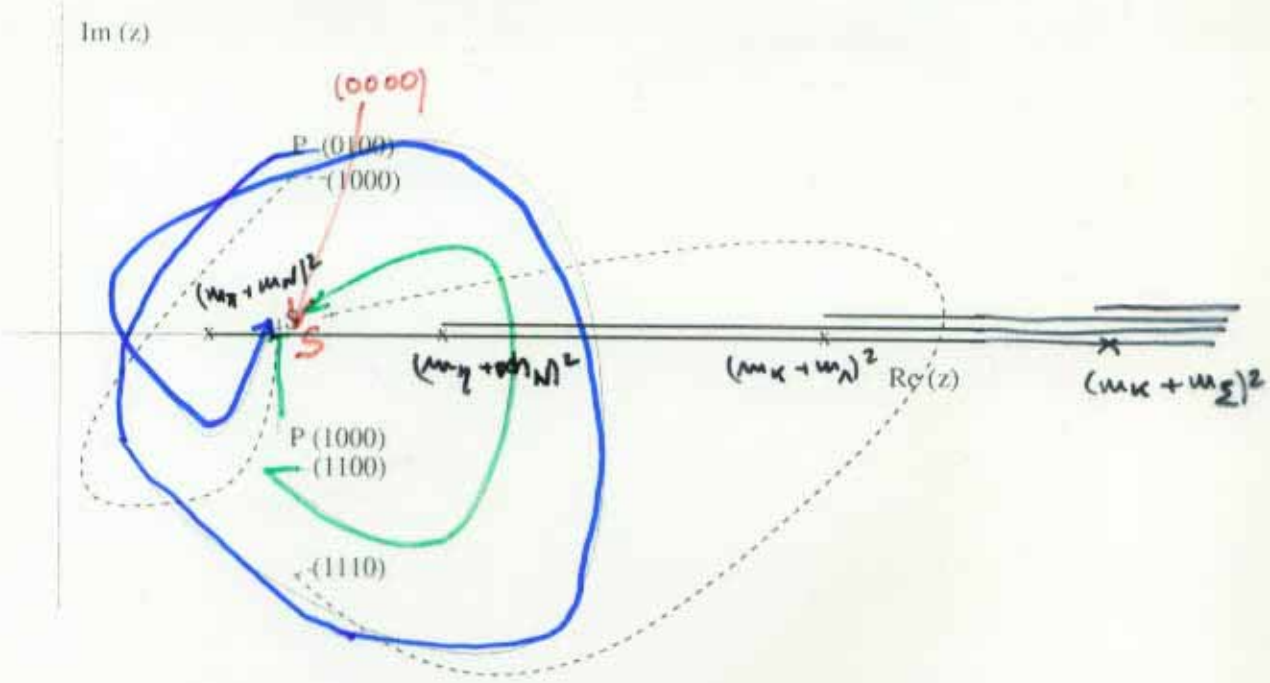

FIG. 6. Different paths, in the $s-$complex plane, showing how to reach the point S, located in the physical scattering region in the interval $[(m_\pi + M_N)^2, (m_\eta + M_N)^2]$, from points P (eventually poles) located in different Riemann sheets, denoted by the vector $\mathbf{n}$ as introduced in Eq. (46), and placed both in the first and fourth quadrants. The unitarity cuts are also depicted in the figure. The "distance" between S and P is obtained by the length of the shortest path joining them. This can be achieved after continuous deformation of the paths depicted in the figure, i.e. any deformations without intersecting the branch points.

Thus, we define the " Second Riemann Sheet" in the relevant fourth quadrant $(t_{II}(s))$ as that which is obtained by continuity across each of the four unitarity cuts. It is obtained using for the diagonal matrix $\bar{J}_0(s)$ the following function[13]

$$\mathcal{L}_{II}(z) = \begin{cases} \mathbf{L}(z;1,0,0,0) & \text{if} \quad (m_\pi + M_N)^2 < \mathrm{Re}(z) < (m_\eta + M_N)^2 \\ \mathbf{L}(z;1,1,0,0) & \text{if} \quad (m_\eta + M_N)^2 < \mathrm{Re}(z) < (m_K + M_\Lambda)^2 \\ \mathbf{L}(z;1,1,1,0) & \text{if} \quad (m_K + M_\Lambda)^2 < \mathrm{Re}(z) < (m_K + M_\Sigma)^2 \\ \mathbf{L}(z;1,1,1,1) & \text{if} \quad (m_K + M_\Sigma)^2 < \mathrm{Re}(z) \end{cases} \tag{47}$$

[13]Though, each of the functions $\mathbf{L}(z;\mathbf{n})$ are analytical in the complex plane, except for the pertinent unitarity cuts, note that $\mathcal{L}_{II}$ so defined, is continuous for real values of s, but presents additional discontinuities out of the real axis.

C. García-Recio
M. J. Vicente-Vacas
E. Ruiz Arriola
J.N.

$\Rightarrow$ Strangeness $S=-1$ } $\bar{K}N, \Sigma\pi, \eta\Lambda, K\Xi$

$I=0$

$L=0$, $J=1/2$, $P=-$ } FOUR COUPLED CHANNELS

DATA. PDG.

$\Lambda(1405)$: $M_R: 1406.5 \pm 4.0$ MeV
$\Gamma_R: 50 \pm 2$

We find:
1443 ± 3, 50 ± 7
$(1368 \pm 12;\ 250 \pm 20)$

Decay Modes $\Sigma\pi$ 100%

$\Lambda(1670)$

$B_{\bar{K}N}: 0.20 \pm 0.05$
$B_{\pi\Sigma}: 0.40 \pm 0.20$
$B_{\eta\Lambda}: 0.25 \pm 0.10$

$M_R: 1670 \pm 10$ MeV
$\Gamma_R: 35^{+15}_{-10}$ MeV. } PDG.

$B_{\bar{K}N}: 0.24$ $B_{\eta\Lambda}: 0.68$
$B_{\pi\Sigma}: 0.08$

1677.5 ± 0.8, 29.2 ± 1.4

$M_R: 1673 \pm 2$ MeV
$\Gamma_R: 23 \pm 6$ MeV } D.M. Manley et al., Phys. Rev. Lett 88 (2002) 012002.

$B_{\bar{K}N}: 0.37 \pm 0.07$
$B_{\pi\Sigma}: 0.16 \pm 0.06$
$B_{\eta\Lambda}: 0.39 \pm 0.08$
$B_{\pi\Sigma^*}: 0.08 \pm 0.06$.

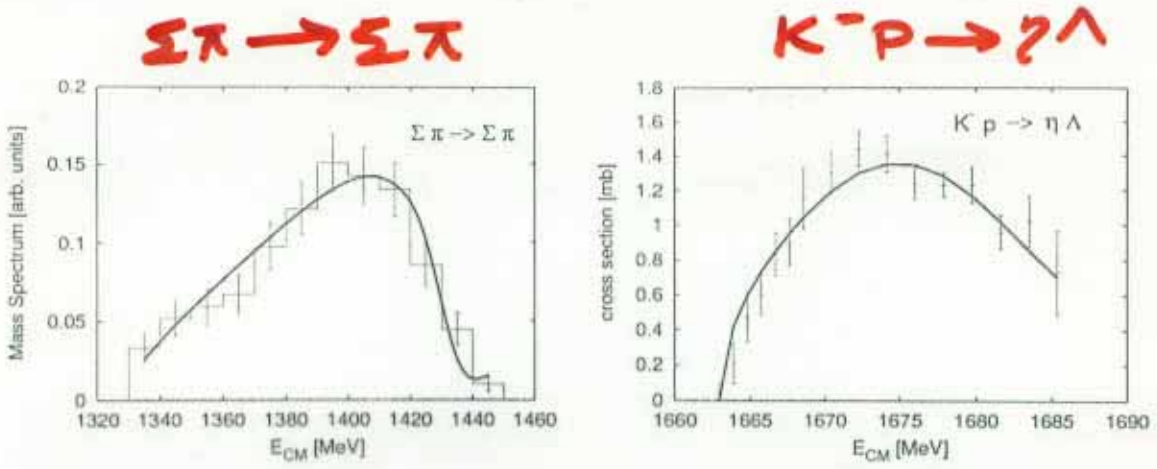

FIG. 1. Solid lines: Results of our calculation. Experimental data for $\pi\Sigma \to \pi\Sigma$ and $K^- p \to \eta\Lambda$ are from Refs. [28] and [30], respectively

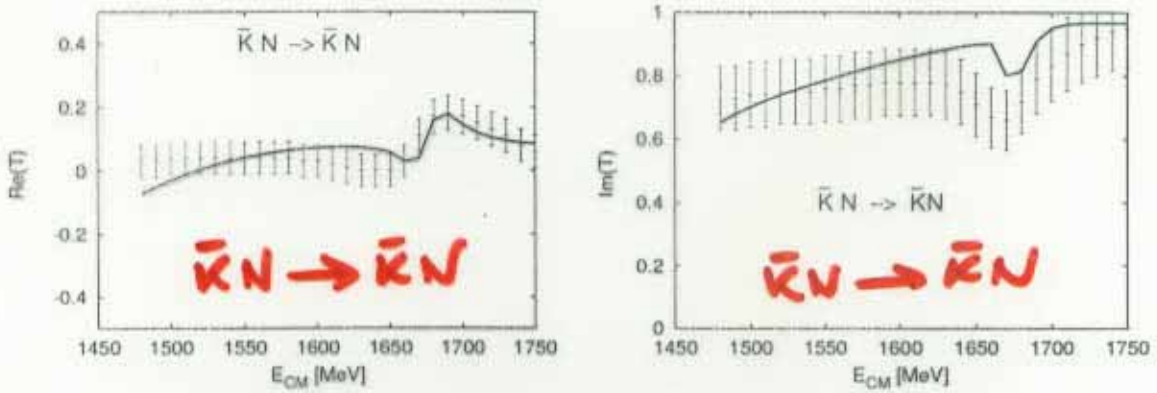

FIG. 2. The real (left panel) and imaginary (right panel) parts of the $s-$wave $T-$matrix, with normalization specified in Eq. (16), for elastic $\bar{K}N \to \bar{K}N$ process in the $I = 0$ isospin channel as functions of the CM energy. The solid line is the result of our calculation, and the experimental data are taken from the analysis of Ref. [26] with the errors stated in the main text.

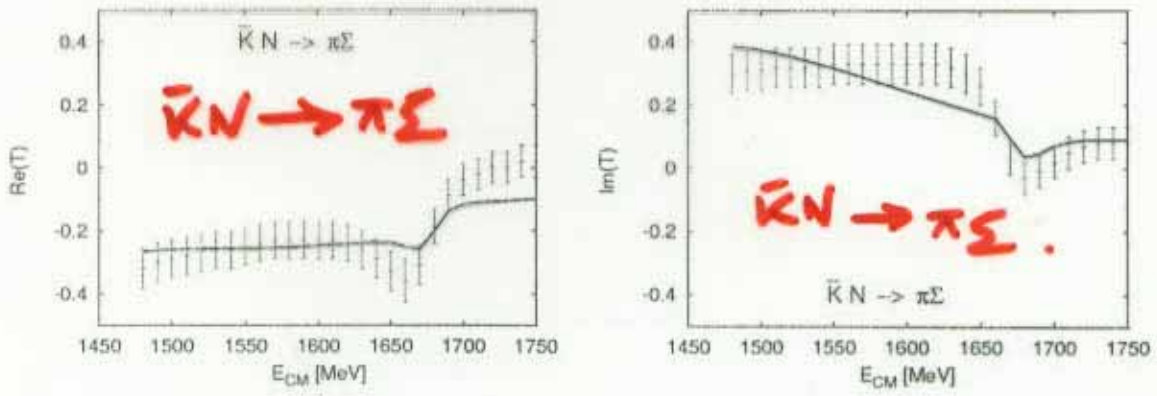

FIG. 3. Same as in Fig. 2 for the inelastic channel $\bar{K}N \to \pi\Sigma$.

For the elastic $\bar{K}N \to \bar{K}N$ scattering length we get

$$a_{\bar{K}N} \equiv \left[f_0^{\frac{1}{2}}(s = (m_K + M_N)^2) \right]_{\bar{K}N \leftarrow \bar{K}N} = (-1.20 \pm 0.09 + \mathrm{i}\ 1.29 \pm 0.09) \quad \text{fm} \tag{19}$$

where the error is statistical and it has been obtained from the covariance matrix given in the Appendix A, taking into account the existing statistical correlations, through a Monte–Carlo simulation. This value should be compared both to the experimental one $(-1.71 + \mathrm{i}\ 0.68)$ fm of Ref. [24] and to the LSE approach of Ref. [17] $(-2.24 + \mathrm{i}\ 1.94)$ fm. Unfortunately, the previous previous works do not provide error estimates, so one cannot decide on the compatibility of results.

C. Second Riemann sheet: poles and resonances.

In this section we are interested in describing masses and widths of the $S_{01}-$ resonances in the $S = -1$ channel. Since causality imposes the absence of poles in the $t(s)$ matrix in the physical sheet [32], one should search for complex poles in unphysical ones. Among all of them, those *closest* to the physical sheet and hence to the scattering line are the most relevant ones. We define the Second Riemann Sheet in the relevant fourth quadrant as that which is obtained by continuity across each of the four unitarity cuts (see a detailed discussion in a similar context in Ref. [21]).

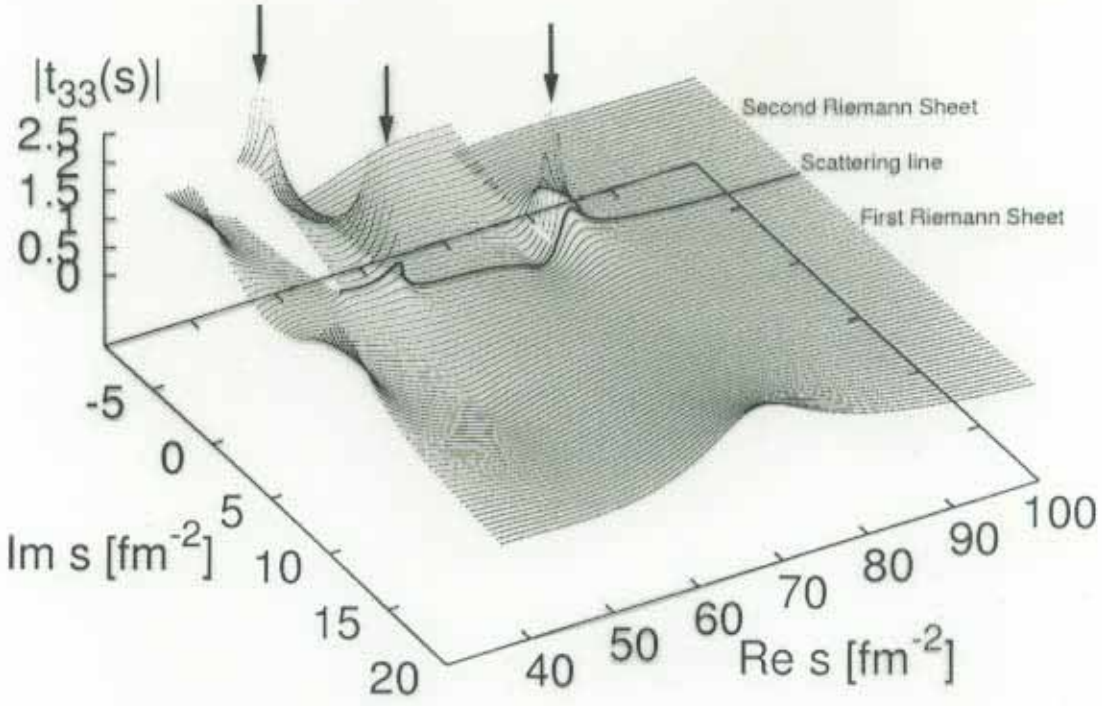

FIG. 4. Modulus of the $\eta\Lambda \to \eta\Lambda$ element of the scattering amplitude $t(s)$ [fm], defined in Eq. (11), analytically extended to the first and fourth quadrants of the $s-$complex plane. The solid line is the scattering line, $s = x + \mathrm{i}\ 0^+$, $x \in \mathbb{R}$, from the first threshold, $(m_\pi + M_\Sigma)^2$, on. The First (Second) Riemann Sheet is depicted in the first (fourth) quadrant of the s complex plane. Three poles appear in the Second Riemann Sheet, which are connected with the $\Lambda(1405)$ and $\Lambda(1670)$ resonances, see discussion in the main text. Besides unphysical poles show up in the physical sheet out of the real axis, but they do not influence the scattering line as can be seen in the plot.

Physical resonances appear in the Second Riemann Sheet of the all matrix elements of $t(s)$, defined in Eq. (11), in the coupled channel space, differing only on the value of the residue at the pole. The residue determines the coupling of the resonances to the given channel. In Fig. 4 we show the absolute value of the $\eta\Lambda \to \eta\Lambda$ element of the t matrix. We choose this channel because all found poles have a sizeable coupling to it. Both the fourth quadrant of the Second Riemann Sheet and the first quadrant of the First (physical) Riemann sheet are shown. The physical scattering takes

Bethe-Salpeter-Equation (BSE)

JN + ERA

Let's consider elastic $\pi\pi$ scattering (NPA 679 (2000) 57)
PLB 455 (1999) 30

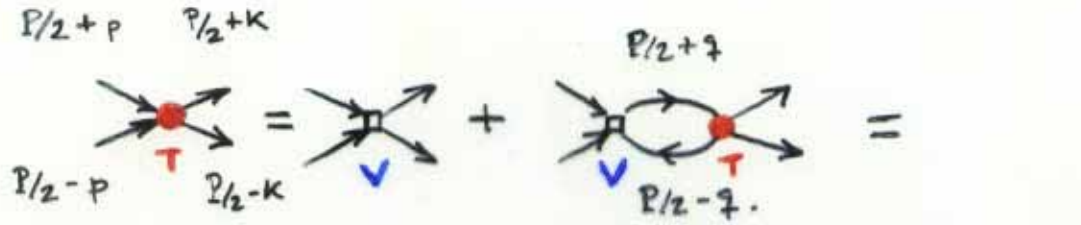

"Sum of bubbles"

$$T_P(p,K) = V_P(p,K) + i\int \frac{d^4q}{(2\pi)^4}\, T_P(q,K)\,\Delta(q_+)\,\Delta(q_-)\,V_P(p,q)$$

$V_P(p,K)$: Two particle irreducible amplitude

$\Delta(q_+)\,\Delta(q_-)$: Exact pseudoscalar meson propagator.

$P^2 = s$,
$q_\pm = P/2 \pm q$

Scattering Amplitude

$$\frac{d\sigma}{d\Omega} = |T_P(p,K)|^2/64\pi^2 s$$

BSE accomplishes two particle unitarity requirement.

$$T_P(p,K) - T_P(K,p)^* = -i(2\pi)^2 \int \frac{d^4q}{(2\pi)^4}\, T_P(q,K)\,\delta^+(q_+^2-m^2)\,\delta^+(q_-^2-m^2)\,T_P(q,P)^*.$$

Given $V \longrightarrow$ BSE generates T which fulfils on- and off-shell unitarity condition.

We propose an expansion (chiral) both for the exact potential (V) and the exact propagator (Δ).

CM phase shifts $\delta_{IJ}(s)$ ← partial wave.
↑ isospin

on-shell.

$$p^2 = k^2 = m^2 - s/4 \quad ; \quad P \cdot p = P \cdot k = 0.$$

$$T_{IJ}(s) = \frac{1}{2} \int_{-1}^{+1} P_J(\cos\theta)\, T^I_P(p,k)\, d(\cos\theta) =$$

$$= \frac{i\, 8\pi s}{\lambda^{1/2}(s, m^2, m^2)} \left[e^{2i\delta_{IJ}(s)} - 1 \right]$$

$$\Delta(p) = \Delta^{(0)}(p) + \Delta^{(2)}(p) + \cdots$$

$$V_P(p,k) = {}^{(0)}V_P(p,k) + {}^{(2)}V_P(p,k) + \cdots$$

INPUT from ChPT

FOR EXAMPLE,

$I=1$, $\pi\pi$ Scattering (p-channel) → LOWEST ORDER

ChpT → $\Delta^{(0)}(p) = \dfrac{1}{p^2 - m^2 + i\epsilon}$

$^{(0)}V_I(p,K) = \dfrac{2p\cdot K}{f^2}$ → on-shell $\dfrac{4m^2 - s}{6f^2}$

T_2

$$T_I^{I=1}(p,K) = \frac{2p\cdot K}{f^2} + i\int \frac{d^4q}{(2\pi)^4} T_I^{I=1}(q,K) \frac{1}{(\frac{p}{2}+q)^2 - m^2 + i\epsilon} \frac{1}{(\frac{p}{2}-q)^2 - m^2 + i\epsilon} \times \frac{2p\cdot q}{f^2}.$$

$$T_I(p,K) = V_I(p,K) + i\int \frac{d^4q}{(2\pi)^4} T_I(q,K)\,\Delta(q_+)\,\Delta(q_-)\,V_I(p,q)$$

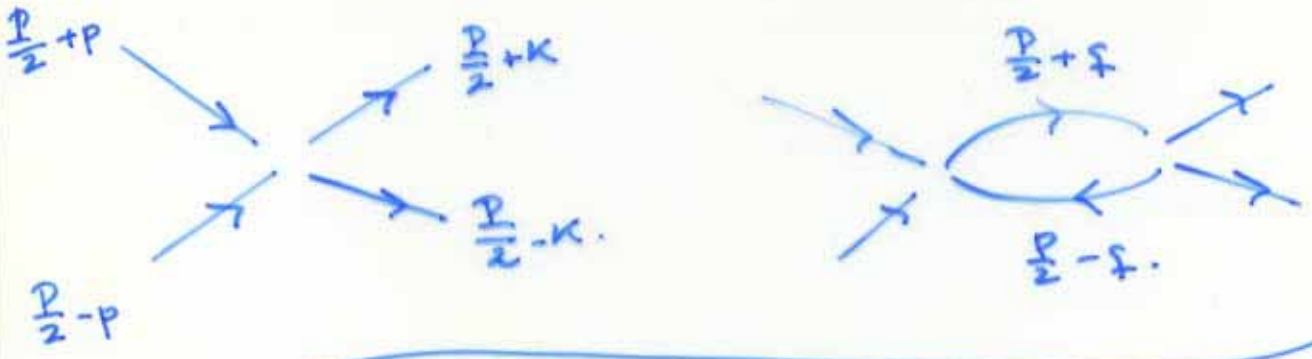

Even for on-shell amplitude $T_I^{I=1}(p,K)$, BSE requires knowledge about off-shell quantities.

One loop. → $T_I^{I=1}(q,K) \approx \dfrac{2q\cdot K}{f^2}$

$$T = \frac{2p\cdot K}{f^2} + i\int \frac{d^4q}{(2\pi)^4}\,\frac{2q\cdot K}{f^2}\,\frac{1}{(P/2+q)^2-m^2+i\epsilon}\,\frac{1}{(P/2-q)^2-m^2+i\epsilon}\,\frac{2P\cdot q}{f^2}$$

$$= \frac{2p\cdot K}{f^2} + \frac{4K_\mu P_\nu}{f^4}\, I^{\mu\nu}.$$

$$I^{\mu\nu} = i\int \frac{d^4q}{(2\pi)^4}\,\frac{q^\mu q^\nu}{(P/2+q)^2-m^2+i\epsilon}\,\frac{1}{(P/2-q)^2-m^2+i\epsilon}$$

$$= A(s)\left\{ g^{\mu\nu} - \frac{P^\mu P^\nu}{s}\right\} + B(s)\, g^{\mu\nu}.$$

$$A(s) = \left[(m^2 - s/4)\, I_0(s) - I_2(4m^2)\right]/3$$

$$B(s) = \frac{1}{2}\, I_2(4m^2)$$

$$I_{2n}(s) = i\int \frac{d^4q}{(2\pi)^4}\,\frac{(q^2)^n}{[q_-^2 - m^2+i\epsilon][q_+^2 - m^2+i\epsilon]}$$

divergent constants — finite

$I_0(s) = \overline{I_0}(4m^2) + \overline{I}_0(s)$ logarithmically divergent → one subtraction

$I_2(s) = \overline{I_2}(4m^2) + (m^2 - s/4)\, I_0(s)$ quadratically

$I_4(s) = \overline{I_4}(4m^2) + (m^2 - s/4)^2\, I_0(s)$ quartically

$$\overline{I}_0(s) = \frac{1}{(4\pi)^2}\sqrt{1-\frac{4m^2}{s}}\,\log\frac{\sqrt{1-\frac{4m^2}{s}}+1}{\sqrt{1-\frac{4m^2}{s}}-1}$$

finite!!

$$T_I(P,K) = \frac{2p\cdot K}{f^2} + \underbrace{[A(s)+B(s)]}_{\text{divergent}}\,\frac{4p\cdot K}{f^4} - \underbrace{A(s)}_{\text{divergent.}}\,\frac{(P\cdot K)(P\cdot p)}{s}\,\frac{4}{f^4}$$

↑ divergent functional

Renormalizable in the Effective Field Theory sense (as ChpT) : Infinite number of counterterms.

Ansatz:

$$T^{I=1}_{I}(p,k) = M(s)\, p\cdot k + N(s)(I\cdot k)(I\cdot p)$$

$$M(s)\, p\cdot k + N(s)(I\cdot k)(I\cdot p) = \frac{2p\cdot k}{f^2} +$$

$$+ i\int \frac{d^4q}{(2\pi)^4}\left\{ M(s)\, q\cdot k + N(s)(I\cdot k)(I\cdot q)\right\} \times$$

$$\times \frac{1}{(P/2+q)^2 - M^2 + i\epsilon}\;\frac{1}{(P/2-q)^2 - M^2 + i\epsilon}\cdot\frac{2p\cdot q}{f^2}$$

$$= \frac{2p\cdot k}{f^2} + \frac{2}{f^2}\left\{ p_\mu k_\nu\, M(s) + N(s)(I\cdot k)\, p_\mu I_\nu \right\} I^{\mu\nu}(s)$$

using $I^{\mu\nu}(s) = A(s)\left\{ g^{\mu\nu} - \frac{P^\mu P^\nu}{s}\right\} + B(s)\, g^{\mu\nu}$

$$M(s) = \frac{2}{f^2} + \frac{2}{f^2}(A+B)\, M(s)$$

$$N(s) = 0 + \frac{2}{f^2}\left\{ -\frac{M(s)}{s}A + N(s)\left\{ (A(s)+B(s)) - A(s)\right\}\right\}$$

System of two equations with two unknowns: $\underline{\underline{M(s), N(s)}}$

$\Rightarrow$ We solve for $M(s)$ y $N(s)$.

$$\left.\begin{matrix} I=1 \\ J=1 \end{matrix}\right\} \rightarrow T_{11}(s) = \frac{s-4m^2}{-6f^2} \frac{1}{1-\left[\frac{-2\tilde{I}_2 + I_0(s)(s-4m^2)}{-6f^2}\right]}$$

$$= \frac{s-4m^2}{-6f^2} + \left\{ \frac{s-4m^2}{-6f^4}\frac{\tilde{I}_2}{3} + \frac{(s-4m^2)^2}{6f^4}\tilde{I}_0 + \frac{s-4m^2}{-6f^2}\bar{I}_0(s)\frac{s-4m^2}{-6f^2} \right.$$

$$\left. + \left\{ \frac{\#}{f^6} + \frac{s-4m^2}{-6f^2}\bar{I}_0(s)\frac{s-4m^2}{-6f^2}\bar{I}_0(s)\frac{s-4m^2}{-6f^2} \right\} + \cdots\cdots \right.$$

$\tilde{I} = I(4m^2)$

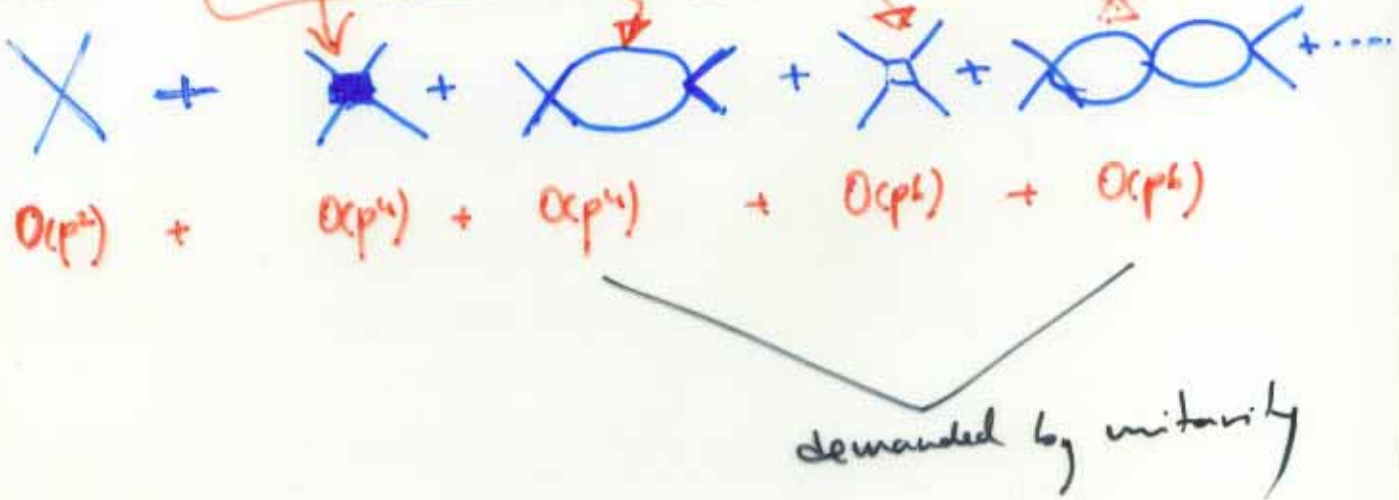

$O(p^2)$ + $O(p^4)$ + $O(p^4)$ + $O(p^6)$ + $O(p^6)$

demanded by unitarity

To Renormalize the amplitudes all possible counterterms should be consider. Thus a counterterm series should be added to the bare amplitude such that the sum of both becomes finite

$$T = V + VGoV + VGoVGoV + \cdots$$

At each order in the perturbative expansion, the divergent part of the counterterm series is completely determined. However, the finite pieces remains arbitrary. Our renormalization scheme is such that the renormalized amplitude can be cast again as

→ Comment on 0098.

→ these parameters can be determined from QCD

→ Std ChpT $O(p^4)$ (SU(2))

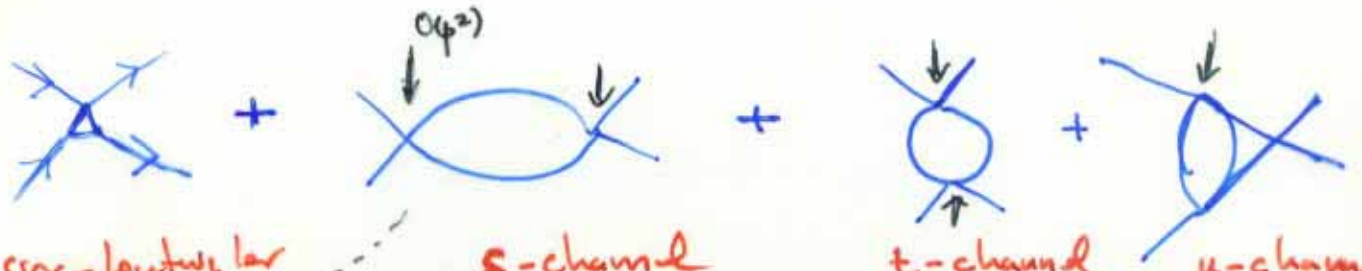

Gasser-Leutwyler counterterms

s-channel

t-channel

u-channel

$$\left(\frac{s-4m^2}{-6f^2}\right)^2 \bar{I}_0(s) + \frac{1}{12f^4}\,\frac{1}{2}\int_{-1}^{+1} d(\cos\theta)\left(f(t)\,\bar{I}_0(t) + f(u)\,\bar{I}_0(u)\right) P_1(\cos\theta)$$

Crossing symmetry

$$+ \mathbb{Q}_2\left((s-4m^2);\ \bar{l}'s\right)$$

LEC's (polynomial of degree two)

Unitarity

→ BSE: If Kernel V is given at order $\frac{1}{f^2}$ →
crossing symmetry is violated at order $\frac{1}{f^4}$

→ Taylor expanding. , we can match

Std ChpT $O(p^4)$ and BSE $O(p^4)$ contribution.

⇓

$I=1,\ J=1$

$$I_0(4m^2) = -\frac{1}{16\pi^2}\left(2(\bar{l}_2-\bar{l}_1)+97/60\right)$$

$$I_2(4m^2) = \frac{m^2}{8\pi^2}\left(2(\bar{l}_2-\bar{l}_1)+3\bar{l}_4-65/24\right)$$

and similarly

$I=0,\ J=0$

$$I_0(4m^2) = -\frac{1}{576\pi^2}\left(22\bar{l}_1+28\bar{l}_2+31/2\right)$$

$$I_2(4m^2) = \frac{m^2}{1440\pi^2}\left(-73+58\bar{l}_1+52\bar{l}_2-72\bar{l}_4\right)$$

$$I_4(4m^2) = \frac{m^4}{7680\pi^2}\left(-172\bar{l}_1-568\bar{l}_2+600\bar{l}_3-672\bar{l}_4+1057\right)$$

$I=2,\ J=0$

$$I_0(4m^2) = \frac{1}{1440\pi^2}\left(43-40\bar{l}_4-160\bar{l}_2\right)$$

$$I_2(4m^2) = \frac{m^2}{2880\pi^2}\left(277+80(\bar{l}_1+\bar{l}_2)-360\bar{l}_4\right)$$

$$I_4(4m^2) = \frac{m^4}{1440\pi^2}\left(189+45\bar{l}_3-180\bar{l}_4\right)$$

→

NOTE $I_0(s) = I_0(4m^2) + \bar{I}_0(s) = i\int\frac{d^4q}{(2\pi)^4}\frac{1}{[q_-^2-m^2+i\epsilon][q_+^2-m^2+i\epsilon]}$

→ divergent → if $\int^{\Lambda^2} d^4s$ → Λ cutoff

Set A

$\bar{l}_1 = -0.62 \pm 0.94$

$\bar{l}_2 = 6.28 \pm 0.48$

$\bar{l}_3 = 2.9 \pm 2.4$

$\bar{l}_4 = 4.4 \pm 0.3$

K_{l4}-decays
Riggenbach + Donoghue + Gasser + Udstein
PRD 43 (1991) 127

Set B

$\bar{l}_1 = -1.7 \pm 1.0$

$\bar{l}_2 = 6.1 \pm 0.5$

$\bar{l}_3 = 2.9 \pm 2.4$

$\bar{l}_4 = 4.4 \pm 0.3$

K_{l4}-decays + $\pi\pi$ 12
Bijnens + Colangelo + Gasser

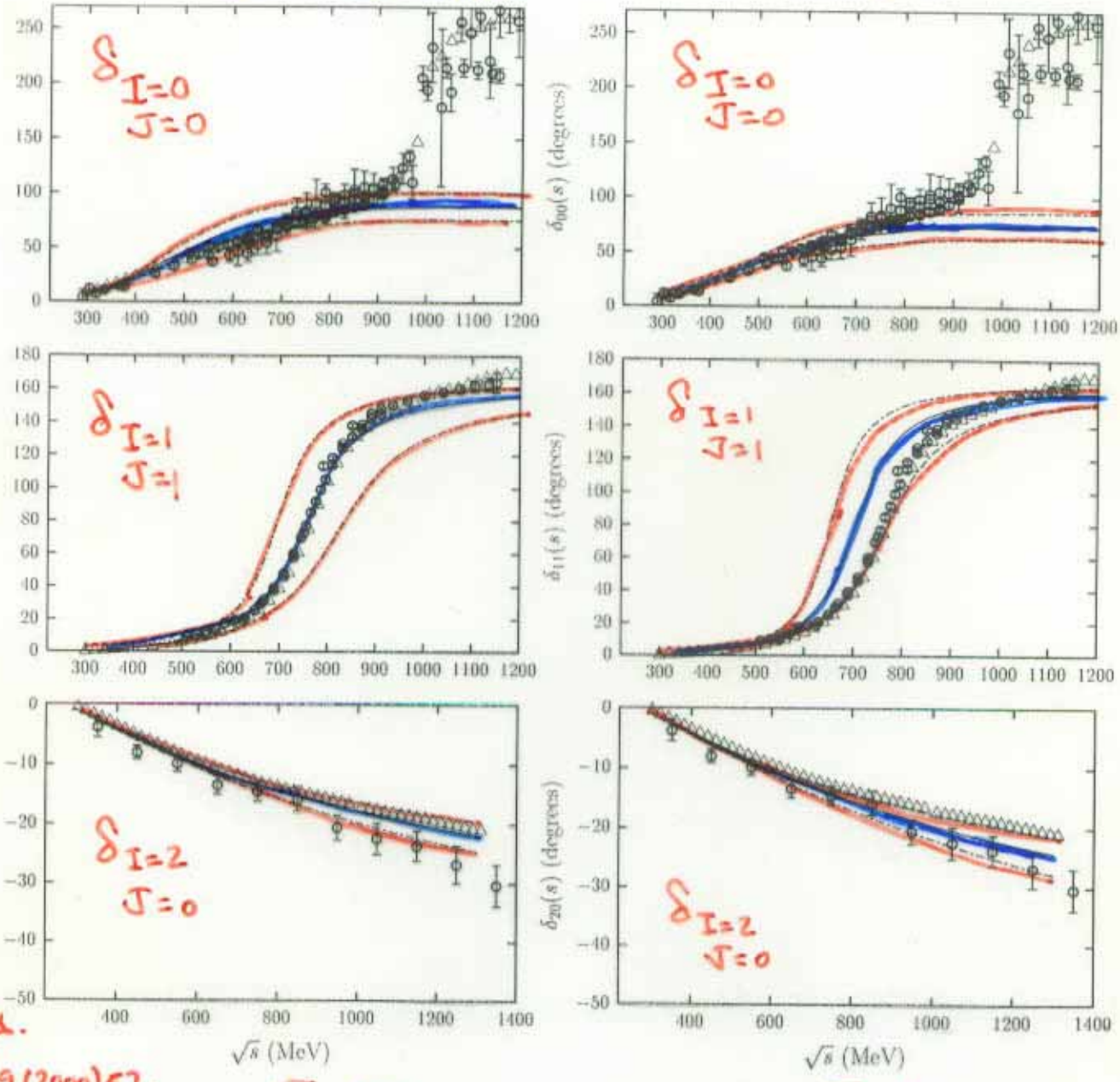

J.W. + ERA.

NPA 679 (2000) 57.

$\sqrt{s}$ MeV.

$\sqrt{s}$ MeV.

FIG. 2. Several $\pi\pi$ phase shifts as a function of the total CM energy $\sqrt{s}$ for both sets of $\bar{l}$'s quoted in Eq. (29). Left (right) panels have been obtained with the set **A** (**B**) of parameters. Solid lines are the predictions of the off-shell BSE approach, at lowest order, for the different IJ–channels. Dashed lines are the 68% confidence limits. Top panels ($I = 0$, $J = 0$): circles stand for the experimental analysis of Refs. [21] - [26]. Middle panels ($I = 1$, $J = 1$): circles stand for the experimental analysis of Refs. [21] and [23]. Bottom panels ($I = 2$, $J = 0$): circles stand for the experimental analysis of Ref. [27]. In all plots the triangles are the Frogatt and Petersen phase-shifts (Ref. [28]) with no errors due to the lack of error estimates in the original analysis.

Set A

$m_\rho = 770^{+90}_{-60}$ MeV

Set B.

715^{+70}_{-50} MeV

bands 68% CL via Monte Carlo simulation